Intrinsic Orbital Angular Momentum States of Neutrons

Ronald L. Cappelletti,[1,*] Terrence Jach,[2] and John Vinson[2]
[1]NIST Center for Neutron Research, National Institute of Standards and Technology, 100 Bureau Drive, Gaithersburg, Maryland 20899, USA
[2]Material Measurement Laboratory, National Institute of Standards and Technology, 100 Bureau Drive, Gaithersburg, Maryland 20899, USA

(Received 20 December 2017; published 2 March 2018)

It has been shown that single-particle wave functions, of both photons and electrons, can be created with a phase vortex, i.e., an intrinsic orbital angular momentum (OAM). A recent experiment has claimed similar success using neutrons [C. W. Clark *et al.*, Nature, **525**, 504 (2015)]. We show that their results are insufficient to unambiguously demonstrate OAM, and they can be fully explained as phase contrast interference patterns. Furthermore, given the small transverse coherence length of the neutrons in the original experiment, the probability that any neutron was placed in an OAM state is vanishingly small. We highlight the importance of the relative size of the coherence length, which presents a unique challenge for neutron experiments compared to electron or photon work, and we suggest improvements for the creation of neutron OAM states.

DOI: 10.1103/PhysRevLett.120.090402

Orbital angular momentum (OAM) or "vortex states" were experimentally realized with photons over 20 years ago [1], and more recently, they have also been created in electron beams [2,3]. These states carry an intrinsic angular momentum that is quantized $\pm l\hbar$ [4]. This intrinsic OAM provides a new degree of freedom, affecting interactions and scattering. A recent paper by Clark *et al.* claimed to demonstrate the creation of quantized orbital angular momentum states in neutron beams [5]. We show here that, because of the very small transverse neutron coherence lengths reported, the claim of Clark *et al.* cannot be supported by their data.

OAM states of matter, currently limited to electron beams, are the subject of significant ongoing research [6,7]. For example, electrons in $l = \pm 1$ OAM states can behave like circularly polarized light when probing condensed matter systems [3]. Additionally, the two-body scattering behavior of particles carrying intrinsic OAM may provide tests of fundamental physics [8]. The creation of neutron OAM states would provide new avenues for testing scattering and increase the utility of thermal neutrons as a structural probe. However, the characteristics of cold neutron sources differ from the electron microscopes or lasers that have heretofore been used in OAM experiments. We begin by reviewing neutron interferometry and the features of the neutron beam. Then we show that the results of Ref. [5] are not sufficient to unambiguously demonstrate an OAM. Given the known properties of the experiment, we show that a negligible number of neutrons were transformed into an OAM state. We conclude by briefly discussing improved OAM detection schemes and the importance of the transverse coherence when designing OAM experiments.

The interferometer used in Ref. [5] follows the well-known Laue-Laue-Laue perfect crystal interferometer design that is used in both neutron [9,10] and x-ray studies [11]. It functions as a Mach-Zehnder interferometer in which an incoming wave packet is split, traverses two separate paths, and then is recombined [12]. The outgoing intensity I_O varies with a path-dependent phase difference $\Delta\varphi(\mathcal{S})$

$$I_O[\Delta\varphi(\mathcal{S})] = A + B\cos[\Delta\varphi(\mathcal{S})], \tag{1}$$

where $\mathcal{S}$ parametrically describes the property giving rise to the phase difference, and A and B are experiment-dependent parameters that govern the observed contrast. For a perfectly machined interferometer, the constants A and B are equal, and the contrast will be 100%. In an experiment, a uniform material is placed in path I, such that the wave packet interacts with it, and phase shifts from this interaction give rise to the measured variations in I_O.

The phase shift $\Delta\varphi(\mathcal{S})$ of a neutron wave packet moving through uniform matter is given by the neutron optics formula [13]

$$\Delta\varphi = -\lambda b N h(\mathcal{S}), \tag{2}$$

where λ is the neutron wavelength, $h(\mathcal{S})$ is the path length through the material, and b and N are the material's coherent neutron-nuclear scattering length and number density, respectively. Combining Eqs. (1) and (2) provides information about the dimensions or composition of the material. However, interference is a single-particle quantum effect, and the intensity in Eq. (1) only gives the probability

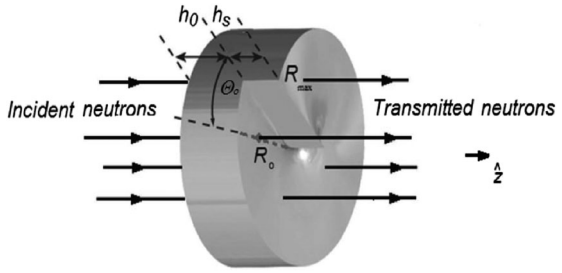

FIG. 1. Schematic diagram of an aluminum spiral phase plate (SPP) used in the Clark *et al.* experiment and based on Fig. 1 of Ref. [5]. The radial and azimuthal coordinates give the surface location of a particular coherent sub-beam within the incoherent mixture of sub-beams. The step height h_s is strongly exaggerated in the figure.

for observing a single neutron. A final phase-contrast image is created by summing the results of many repeated single-neutron interference measurements.

Cold neutrons coming from a reactor, e.g., the NIST Center for Neutron Research facility used in Ref. [5], and Bragg-reflecting from a pyrolytic graphite monochromating crystal have coherence lengths of several tens of nm in the vertical direction, of order 5,000 nm in the horizontal direction [14], and about 20 nm in the longitudinal direction [15,16]. A recent experiment showed that the vertical coherence length in the NIST interferometer instrument is about 80 nm [17], yielding an approximate transverse coherence area of 0.4×10^6 nm^2. The cross sectional area of the neutron beam depends on the experimental arrangement, but it is of order 0.5 cm^2 $= 0.5 \times 10^{14}$ nm^2. An individual neutron, therefore, samples approximately 10^{-8} of the area of the total beam. At a nominal flux of 10^7 neutrons per cm^2 s, the mean distance between neutrons is approximately 4 cm. The coherence size and flux of the neutrons ensure that each neutron interferes only with itself. An interferometry image is generated by collecting many single-neutron results, where each subsequent neutron travels a parallel path $\mathcal{S}$, randomly offset within the beam.

The Clark *et al.* experiment involved placing various aluminum spiral "ramp" phase plates (SPP) (see Fig. 1) into one leg of the interferometer. These objects had diameters ranging from 10–15 mm and step thicknesses h_s of 112, 224, and 840 μm. The SPP thickness varies linearly with azimuthal angle about the center of the SPP as

$$h(\Theta) = h_0 + h_s \frac{\Theta}{2\pi}. \tag{3}$$

A device (phase flag) is included in the interferometer to cancel any parts of the phase difference not arising from the angular term in Eq. (3). In the experiment, the neutrons had a kinetic energy of 11.14 meV, corresponding to a wavelength of 0.271 nm. The monochromaticity $(\Delta\lambda/\lambda)$ of this beam is approximately 0.25 percent. The scattering length of aluminum is 3.449 fm [18], and the atom density is 6.030×10^{22} cm^{-3}. Thus, according to Eq. (2), the phase shift corresponding to a step height h_s of 112 μm is $\Delta\varphi_s = 6.312$ rad $\approx 2\pi$. The other SPPs were machined to approximate net phase variations of various integral or half-integral multiples of 2π.

By construction, the phase shift $\Delta\varphi_s$ along $\mathcal{S}$ depends on the azimuthal angle Θ of the SPP, and correspondingly, the intensity I_O is given, apart from a constant phase difference, which can be adjusted to zero by

$$I_O[\Theta] = A + B\cos[(\lambda b N h_s/2\pi)\Theta]. \tag{4}$$

The parameter $\lambda b N h_s/2\pi$ is at the experimenters' disposal, since it depends on the material and step height chosen. We define $M \equiv \lambda b N h_s/2\pi$, giving

$$I_O[\Theta] = A + B\cos[M\Theta], \tag{5}$$

where M can be an any real number, including an integer, depending upon the design of the SPP placed in the interferometer. For example, suppose that two SPPs are placed sequentially in the beam path, one with a step thickness $h_s = 112$ μm and a second one with a step thickness 224 μm, then the variation of the intensity as a function of azimuthal angle would be given by

$$I_O[\Theta] = A + B\cos[3\Theta], \tag{6}$$

such that the intensity pattern on the screen would show 3 lobes, completely describing the image displayed in Fig. 4 of Ref. [5].

All of the other two-dimensional intensity maps therein can be explained in an analogous manner: phase contrast images of the thickness of the SPPs. Phase contrast imaging is well known for both x-rays [19] and neutrons [20]. The images arise directly as a consequence of Eq. (5), but the parameter M is a continuous real number related to the step height. The images can be accounted for without requiring any reference to OAM states. Therefore a different experimental measurement is required to confirm a neutron OAM.

Spiral phase plates have been used successfully in optical experiments to create OAM states with laser beams [21,22]. While the neutron and photon SPP experiments appear to be analogous, the difference in relative transverse coherence is crucial. In the case of a laser beam, each photon has a transverse coherence length that is on the same scale as the phase plate and beam diameters, whereas the neutron wave packets are relatively nanoscopic. As we will show, creating an OAM state with an SPP requires a transverse coherence length comparable to the beam and SPP diameters.

A possible reason for the interpretation given by Clark *et al.* of the images constituting their data comes from the following considerations. Each neutron will experience a

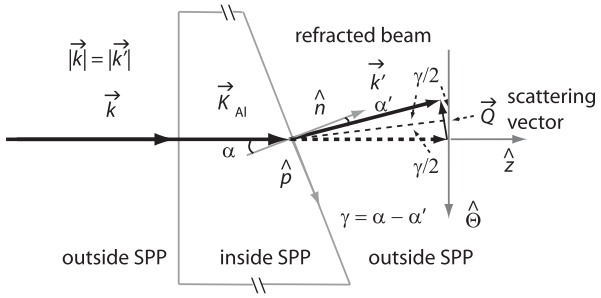

FIG. 2. Neutron optical ray diagram showing the refraction of a ray leaving the SPP surface at angle α' having entered it at incident angle α. The scattering angle is $\gamma = \alpha - \alpha'$. The scattering vector $|\vec{Q}| = 2k\sin(\gamma/2)$ has a component in the $-\hat{\Theta}$ direction of $Q_\Theta = -k\sin(\gamma)$, representing an azimuthal impulse given to the neutron by the SPP.

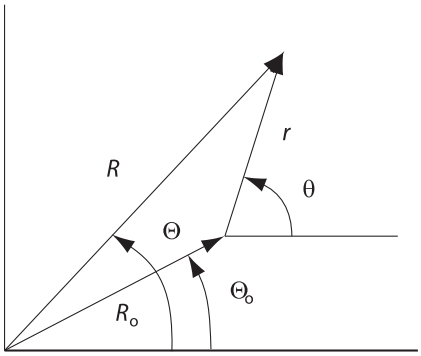

FIG. 3. Relationship between local wave function coordinates (r, θ) and SPP coordinates (R, Θ) for a neutron centered at (R_0, Θ_0) emerging from the SPP. The thick line is the raised step, looking at the SPP towards the $-\hat{z}$ direction.

transverse impulse in momentum $p_\Theta = \hbar Q_\Theta$ in the azimuthal $-\hat{\Theta}$ direction upon exiting the SPP as shown in Fig. 2. The scattering angle in Fig. 2, for small angles of incidence and refraction (i.e., for $R > 100$ nm), is given by $\gamma \approx (\lambda^2 bN)h_s/(4\pi^2 R)$, such that the value of the angular momentum about the SPP axis arising from this impulse is

$$L_z^{\mathrm{SPP}} \approx -\hbar R\frac{\lambda bNh_s}{2\pi R} = -\hbar M, \tag{7}$$

which is independent of R in the stated limit of small scattering angle. An integral value of M may be selected by judicious construction of the SPP, giving this angular momentum the appearance of a quantum effect. However, Eq. (7) is equally valid for rays with no vortex or OAM character.

Next, we evaluate the expectation value of the intrinsic angular momentum for a single neutron wave packet that has passed through the SPP. We begin by modeling an incident neutron striking the SPP off axis, centered at (R_0, Θ_0), in the paraxial approximation, namely the direction of propagation differs little from the $\hat{z}$ direction. Within the paraxial approximation, Laguerre-Gaussian (LG) beams provide a complete basis with well-defined orbital angular momentum [7]. We assume that the incident wave packet has no OAM, and we use the $(l = 0, n = 0)$ LG solution. We take the minimum beam waist to be ξ_T, the transverse coherence length (taken for simplicity to be a single parameter). Our calculations show that the radius of curvature of the wave front is slowly varying and nearly infinite, and hence, the beam waist changes little within the interferometer. Therefore, the transmitted transversely-normalized wave function is

$$\psi_t(r,\theta,z) = \frac{\sqrt{2/\pi}}{\xi_T}e^{-r^2/\xi_T^2}e^{ikz}e^{-iM\Theta(r,\theta)}, \tag{8}$$

where the wave packet has acquired a position-dependent phase $M\Theta(r,\theta)$ from the SPP.

Using this wave function, we can calculate the expectation values of the angular momentum about the center of the packet, i.e., the intrinsic OAM.

$$\begin{aligned}\langle L_z\rangle_{R_0} &= \langle\psi_t|\left(-i\hbar\frac{\partial}{\partial\theta}\right)|\psi_t\rangle \\ &= \frac{-2}{\pi\xi_T^2}\hbar M\int_0^\infty rdre^{\frac{-2r^2}{\xi_T^2}}\int_0^{2\pi}d\theta\frac{\partial\Theta(r,\theta)}{\partial\theta}.\end{aligned} \tag{9}$$

The angular integral can be easily evaluated by examining Fig. 3. As the angle θ undergoes its excursion during integration, the angle $\Theta(r,\theta)$ also varies. So long as $r < R_0$ the net excursion of Θ is zero, but when $r > R_0$, Θ undergoes a 2π excursion as θ does. Hence the angular integral is $2\pi H(r - R_0)$, where H is the Heaviside function. Incorporating the Heaviside function into the radial integral, we have:

$$2\pi\int_{R_0}^\infty rdre^{\frac{-2r^2}{\xi_T^2}} = 2\pi\frac{\xi_T^2}{4}e^{\frac{-2R_0^2}{\xi_T^2}}. \tag{10}$$

Our result for the expectation value of the intrinsic OAM for ψ_t is

$$\langle L_z\rangle_{R_0} = -\hbar Me^{\frac{-2R_0^2}{\xi_T^2}}. \tag{11}$$

We can arbitrarily distinguish this to be a substantial probability for a neutron acquiring OAM when the value of R_0 is such that the exponential term is $\geq e^{-0.5}$. Using this criterion, for a transverse coherence length of $\xi_T = 5,000$ nm and a beam radius of 0.5 cm, about one in a million neutrons would acquire an OAM in the Clark *et al.* experiment. Conversely, if the transverse coherence length of the beam were comparable to the radius of the SPP or the neutron beam, this expression shows that the expectation value of the OAM about the c.m. axis for each neutron would approach $-\hbar M$. The vast majority of neutrons would be in quantized OAM states with an angular momentum of $-\hbar M$, as in optical experiments.

For the wave function in Eq. (8), we calculate the expectation value of the total angular momentum about the SPP axis (which includes the angular momentum about the c.m. axis) by replacing the angular derivative in the operator by $(\partial/\partial\Theta)$. In doing so, we recover the result obtained by the refraction method in Eq. (7) above, namely $\langle L_z \rangle_{\mathrm{SPP}} = -\hbar M$. However, this extrinsic angular momentum relative to the SPP axis varies continuously with M and has no quantum character.

In conclusion, the 2D patterns observed in the Refs. [5] and [23] can be understood as simply arising from the interference intensity given by Eq. (5), with no reference to the intrinsic OAM. While an alternative way of interpreting the observed interference patterns is to think of M as characterizing the angular momentum about the SPP axis, this angular momentum is not quantized, and moreover, it does not arise from a twisted wave front associated with a vortex wave. Hence, it is not a relevant physical quantity available to be transferred in subsequent interactions of the neutron with other systems. The important physical quantity is the intrinsic OAM, i.e., that gained by a neutron wave packet about its center of momentum. A model calculation gives a vanishingly small value of the expectation value of this OAM for the vast majority of incident neutrons because of the small transverse coherence of their wave functions.

Crucially, the interferometry measurements of Clark *et al.* are unable to distinguish between the case at hand, where a macroscopic beam of neutrons having small transverse coherence interrogates the phase contrast of the SPP, versus a beam of macroscopically transversely coherent neutrons in OAM states. This is clear from Eq. (11) in the limit of a large coherence length ξ_T. The creation of neutron OAM states could be tested using a method analogous to Ref. [24] or through scattering or decay measurements. The OAM carried by the individual neutrons would be conserved both in magnitude and direction through the reaction, changing the energies or spatial distributions of the end products.

The small transverse coherence length of the neutron beam is the primary barrier to the creation of neutron OAM states. As we have shown, the method used by Clark *et al.* would be effective if the incoming neutron beam were coherent across the diameter of the beam. In principle, improved transverse coherence can be achieved, at the cost of flux, by placing a pinhole in the beam with a SPP placed sufficiently downstream for the wave function to have expanded transversely to cover it. Alternatively, different schemes for generating monochromatic neutron beams may provide sufficient coherence [25].

We want to thank Jeffrey Lynn, Rob Dimeo, and Chuck Majkrzak for useful and important conversations. Also, more than a year ago, Sam Werner pointed out that the 2D images displayed in Ref. [5] are actually phase contrast images of the thickness profiles of the SPPs, having no direct connection to orbital angular momentum.

*ronald.cappelletti@nist.gov

[1] L. Allen, M. W. Beijersbergen, R. J. C. Spreeuw, and J. P. Woerdman, Phys. Rev. A **45**, 8185 (1992).
[2] M. Uchida and A. Tonomura, Nature **464**, 737 (2010).
[3] J. Verbeeck, H. Tian, and P. Schattschneider, Nature **467**, 301 (2010).
[4] A. T. O'Neil, I. MacVicar, L. Allen, and M. J. Padgett, Phys. Rev. Lett. **88**, 053601 (2002).
[5] C. W. Clark, R. Barankov, M. G. Huber, M. Arif, D. G. Cory, and D. A. Pushin, Nature **525**, 504 (2015).
[6] S. M. Lloyd, M. Babiker, G. Thirunavukkarasu, and J. Yuan, Rev. Mod. Phys. **89**, 035004 (2017).
[7] K. Y. Bliokh, I. P. Ivanov, G. Guzzinati, L. Clark, R. V. Boxem, A. Béché, R. Juchtmans, M. A. Alonzo, P. Schattschneider, F. Nori, and J. Verbeeck, Phys. Rep. **690**, 1 (2017).
[8] I. P. Ivanov, D. Seipt, A. Surzhykov, and S. Fritzsche, Phys. Rev. D **94**, 076001 (2016).
[9] H. Rauch, W. Treimer, and U. Bonse, Phys. Lett. **47A**, 369 (1974).
[10] H. Rauch and S. A. Werner, *Neutron Interferometry: Lessons in Experimental Quantum Mechanics, Wave-Particle Duality, and Entanglement*, 2nd ed. (Oxford University Press, Oxford, 2015).
[11] U. Bonse and M. Hart, Appl. Phys. Lett. **6**, 155 (1965); **7**, 238 (1965).
[12] We are indebted to Prof. Samuel A. Werner for a detailed discussion of how the LLL interferometer actually works in practice, taking account of the small transverse coherence lengths of the incident neutrons, and for the role of phase contrast images in Ref. [5].
[13] See Eq. (2.6) on p. 29 of Ref. [10].
[14] H. Rauch, H. Wolwitsch, H. Kaiser, R. Clothier, and S. A. Werner, Phys. Rev. A **53**, 902 (1996).
[15] H. Kaiser, S. A. Werner, and E. A. George, Phys. Rev. Lett. **50**, 560 (1983).
[16] C. F. Majkrzak, C. Metting, B. B. Maranville, J. A. Dura, S. Satija, T. Udovic, and N. F. Berk, Phys. Rev. A **89**, 033851 (2014).
[17] D. A. Pushin, M. Arif, M. G. Huber, and D. G. Cory, Phys. Rev. Lett. **100**, 250404 (2008).
[18] See the table of scattering lengths on p. 65 of Ref. [10].
[19] A. Momose, Opt. Express **11**, 2303 (2003).
[20] F. Dubus, U. Bonse, M. Zawisky, M. Baron, and R. Loidl, IEEE Trans. Nucl. Sci. **52**, 364 (2005); See also Sec. 9.2.4 of Ref. [10].
[21] M. Massari, G. Ruffato, M. Gintoli, F. Ricci, and F. Romanato, Appl. Opt. **54**, 4077 (2015).
[22] A. M. Yao and M. J. Padget, Adv. Opt. Photonics **3**, 161 (2011).
[23] D. Sarenac, M. G. Huber, B. Heacock, M. Arif, C. W. Clark, D. G. Cory, C. B. Shahi, and D. Pushin, Opt. Express **24**, 22528 (2016).
[24] J. Leach, M. J. Padgett, S. M. Barnett, S. Franke-Arnold, and J. Courtial, Phys. Rev. Lett. **88**, 257901 (2002).
[25] A. G. Wagh, S. Abbas, and W. Treimer, Nucl. Instrum. Methods Phys. Res., Sect. A **634**, S41 (2011).